# Equation of state of $N_2$ and Ne near their critical points. Scaling, corrections to scaling, and amplitude ratios

M. W. Pestak* and M. H. W. Chan
*Department of Physics, The Pennsylvania State University, University Park, Pennsylvania 16802*
(Received 28 October 1983)

Five stacked parallel plates forming four capacitors were used to measure the density at four different heights for nitrogen and neon near their critical points. Measurements were made on fluid samples with an average density very close to the critical value in a temperature range $-5\times10^{-2}<t<1\times10^{-3}$ where $t$ is the reduced temperature $(T-T_c)/T_c$. These measurements allow simultaneous determinations of (1) the coexistence curve, (2) isothermal compressibility both in one-phase ($T>T_c$) and the two-phase region ($T<T_c$), and (3) the density as a function of chemical potential of these fluids. For data outside the gravitationally rounded region, power-law analyses including correction to scaling terms were used. Data in the gravitationally rounded region were analyzed with the use of the restricted cubic model. Consistent results in $T_c$ (on the order of 0.2 mK) and the leading amplitudes were found between data in these two regions. In addition to the leading exponent $\beta$ and $\gamma$ we also determined from our data the correction to scaling exponent $\Delta$ and three universal amplitude ratios. Our values for these quantities are in good agreement with theoretical predictions.

## I. INTRODUCTION

A bulk pure fluid near its liquid-vapor critical point is commonly believed to fall in the same universality class as the three-dimensional Ising model[1] or the Landau-Ginsburg-Wilson model with a scalar order parameter.[2] On the coexistence curve below the critical temperature $T_c$, if the average of the liquid and vapor densities is the critical density ($\rho_L+\rho_V=2\rho_c$), then the order parameter is described by

$$\Delta\rho^*=B_0\,|\,t\,|^{\beta}\,, \tag{1}$$

where $\Delta\rho^*=(\rho_L-\rho_V)/(2\rho_c)$, $t=(T-T_c)/T_c$ is the reduced temperature, and $\beta$ is a universal critical exponent. The simple power law is expected to be valid only in the asymptotic critical region (i.e., sufficiently close to the critical point). The value of $\beta$ is predicted to be 0.325 by renormalization-group (RG) theory.[3,4] The value of $\beta$ found in recent high-temperature-series— (HTS) expansion calculations is converging toward the RG values.[5,6] $B_0$ is a system-dependent amplitude.

Similarly, the dimensionless isothermal compressibility $\chi_T=(P_c/\rho_c^2)(\partial\rho/\partial\mu)_{T'}$ as a function of reduced temperature, asymptotically becomes

$$\chi_T^{\pm}=\Gamma_0^{+}t^{-\gamma^+}\,. \tag{2}$$

The value of $\gamma^+$ is predicted to be 1.240 by RG ($\pm0.002$) (Refs. 3 and 4) and HTS calculations.[5–7] This expression applies above $T_c$ on the critical isochore. An expression identical to Eq. (2) with negative ($-$) superscripts applies along the coexistence curve. The $\Gamma$'s are system-dependent amplitudes.

Also of interest is the relation between the reduced chemical potential,

$$\Delta\mu^*=(\rho_c/P_c)[\mu(\rho,T)-\mu(\rho_c,T)]\,, \tag{3}$$

and the reduced density on the critical isotherm

$$|\,\Delta\mu^*\,|=D_0\,|\,(\rho-\rho_c)/\rho_c\,|^{\delta}\,, \tag{4}$$

where the value of $\delta$ is predicted to be 4.82. $D_0$ is the associated amplitude. Among the many power laws and critical exponents, the three listed above are of particular interest to the experimental work to be presented here. Not all the critical exponents are independent; they are related by scaling relations[8] such that knowledge of any two exponents allows the determination of all the others. The exponent relations of particular interest here are $\gamma=\beta(\delta-1)$ and $\gamma^+=\gamma^-$.

The experiment of Hocken and Moldover,[9] performed inside $|\,t\,|<5\times10^{-5}$, found critical exponents in much better agreement with the predicted values than those found in many previous experiments performed farther from $T_c$.

It was recognized in the early 1970s that the true asymptotic critical region is exceedingly small and therefore inaccessible to most experiments. Equations (1), (2), and (4) need to be modified by adding correction-to-scaling terms[10] to properly describe data that extend outside the asymptotic critical region. The detailed expressions for pure fluids have been worked out by Ley-Koo, Green, and Sengers[11,12] following Wegner's expansion.[10] The extended forms for Eqs. (1), (2), and (4), are, respectively,

$$\Delta\rho^*=B_0\,|\,t\,|^{\beta}(1+B_1\,|\,t\,|^{\Delta}+B_2\,|\,t\,|^{2\Delta}\cdots)\,, \tag{5}$$

$$\chi_T^{\pm}=\Gamma_0^{+}t^{-\gamma^+}(1+\Gamma_1^{+}t^{\Delta}+\Gamma_2^{+}t^{2\Delta}\cdots)\,, \tag{6}$$

$$|\,\Delta\mu^*\,|=D_0\,|\,(\rho-\rho_c)/\rho_c\,|^{\delta}\times[1\pm D_1\,|\,(\rho-\rho_c)/\rho_c\,|^{\Delta/\beta}+\cdots]\,. \tag{7}$$

 

The correction amplitudes $B_1$, $B_2$, $\Gamma_1^+$, $\Gamma_2^+$, and $D_1$ are system-dependent quantities. The first correction exponent $\Delta$ has been calculated to be $0.493\pm0.007$ by RG methods.[4] The HTS values for $\Delta$ are found in two recent calculations to be $0.49\pm0.08$ (Ref. 6) and $0.54\pm0.05$.[7] The value of the second correction exponent is less certain, but has been estimated to be 0.9.[13] We make the assumption that the second correction exponent is equal to $2\Delta$.[12]

The experimental evidence for the existence of such correction terms first surfaced in 1969. If a simple power law was assumed, the order-parameter exponent value in Xe was found to depend upon the temperature range of data being analyzed.[14] This behavior was confirmed in $SF_6$ in 1972,[15] and in other experiments subsequently.[16–18] The need for a correction-to-scaling term was also found in a study of superfluid densities of $^4$He under pressure.[19]

Consistency with the correction-to-scaling terms is usually demonstrated by fixing the value of $\Delta=0.5$ and the leading exponents at their RG values. This way of analyzing experimental data yields a better fit (or as good a fit) than analysis in terms of a simple power law with effective exponents.[17,18,20]

Direct experimental determination of the correction exponent $\Delta$ requires extremely precise density measurements on the coexistence curve. If $B_1$ of Eq. (5) is on the order of unity then the correction term $B_1|t|^{\Delta}$ makes a contribution of only about 3% to the order parameter at a reduced temperature of $t=1\times10^{-3}$. Ley-Koo and Green[21] reanalyzed the previously obtained data on $SF_6$ (Ref. 22) and found $\Delta$ to be $\sim0.52$. The uncertainty in $\Delta$ was found to be dependent on the procedures adopted, and varies between 0.04 and 0.20. Beysens and Bourgou[23] found $\Delta=0.52\pm0.03$ in their binary-fluid experiments. There is, however, some concern with their procedure of data reduction.[24,25] Our results, which are discussed below, offer strong evidence that $\Delta$ is in fact near 0.5.

Scaling not only predicts relations between the critical exponents, but also predicts that specific (system-dependent) amplitudes should maintain universal amplitude ratios.[26–28] The three amplitude ratios that we measure are $\Gamma_0^+D_0B^{\delta-1}$, $\Gamma_0^+/\Gamma_0^-$, and $B_1/\Gamma_1^+$. These predictions have been examined in a number of papers[18,26,28–30] by combining results from different experiments. These "experimental" values of the ratios are not reliable since it is exceedingly difficult if not impossible to detect and eliminate inconsistencies in the experimental conditions and in the procedures adopted for data analysis in the different experiments.[26] The amplitudes, for example, are very sensitive to the choice of $T_c$. In order to test these ratios properly, the appropriate amplitudes should be determined consistently and independently in a single experiment. Amplitude ratios obtained from a data analysis that assumes specific parametric models of equation of state are also not suitable, since in these models the amplitude ratios are either built in or implied.[29–31] We know of very few experiments where these amplitude ratios were determined with the above-mentioned bias-free procedures. For pure fluids, the ratio $\Gamma_0^+/\Gamma_0^-$ was measured by Weber[32] on $O_2$ and Wallace and Meyer[33] on $^3$He. The only determination of the correction amplitude ratio to date is by Pittman, Doiron, and Meyer[17] on $^3$He. The values found by these workers shall be compared with our results and with theoretical predictions in Sec. IV. We know of no determination of the ratio $\Gamma_0^+D_0B_0^{\delta-1}$. A careful experimental examination of these commonly believed universal ratios is clearly needed.

In Pittman's experiment, the order parameter and the isothermal compressibility are measured simultaneously with three parallel plates forming two capacitors. Weber[32] used a stack of five capacitors spanning a total height of over 10 cm in his sample cell. The gravitational-rounding effect[34,35] is a severe constraint in Weber's experiment. In this experiment we improve upon the parallel-capacitance-plate technique discussed above. Our sample cell has five plates stacked together, forming four parallel-plate capacitors (Fig. 1). This allows us to measure the density at four different values of the chemical potential as a function of temperature. Below $T_c$ the lower two capacitor gaps measure the liquid density and the upper two measure the vapor density. Above $T_c$ the density difference between any two capacitor gaps is a measure of the isothermal compressibility [Eq. (6)]. Our coexistence-curve data are sufficiently precise to allow direct determination of not only the value of $\beta$, but also the first correction to scaling exponent $\Delta$ of Eq. (5). Since there are four capacitors, we can measure the density twice in the liquid and twice in the vapor at different values of the chemical potential, and determine the two-phase compressibility [Eq. (6) with negative superscripts]. On the critical isotherm we determine the chemical potential versus density [Eq. (7)]. This experiment yields a total of four independent leading amplitudes ($B_0$, $\Gamma_0^+$, $D_0$, and $\Gamma_0^-$) and two correction amplitudes ($B_1$ and $\Gamma_1^+$). Combining the appropriate amplitudes, we obtain values for all three universal amplitude ratios mentioned above. The total height of the five parallel plates is kept under 1.2 cm to reduce the gravitational-rounding effects.

The design of the sample cell gives important information (which is lacking in most earlier experiments) about gravitational rounding and temperature gradients.[35] The former must be properly considered in the analysis, while the latter must be eliminated. We report in this paper an exhaustive study on nitrogen and neon. Data acquisition continued, without warming the cryostat up to room temperature, for 15 months—more than 2300 data points were collected. The majority of the information is on the $N_2$ system because we initially gathered data with intentionally imposed temperature gradients to thoroughly understand their effect on our measurements. In addition to $N_2$ and Ne, we have also made equation-of-state measurements of HD near its critical point. We found the time required to establish hydrostatic equilibrium in HD is about a factor of 4 longer than the other two fluids. Near $T_c$, up to 8 h per data point are needed. Since retransfer of He is required every 5 d, and each transfer tends to disrupt the hydrostatic equilibrium of the sample, we gathered far less data points for HD than for $N_2$ and Ne. Whereas the results we found for such quantities as $\beta$, $\gamma$, $B_0$, and $\Gamma_0$ for HD are equally reliable as the ones reported here for $N_2$ and Ne, quantities such as $\Delta$, $\Gamma_0^-$, and correction amplitudes that require more data points,

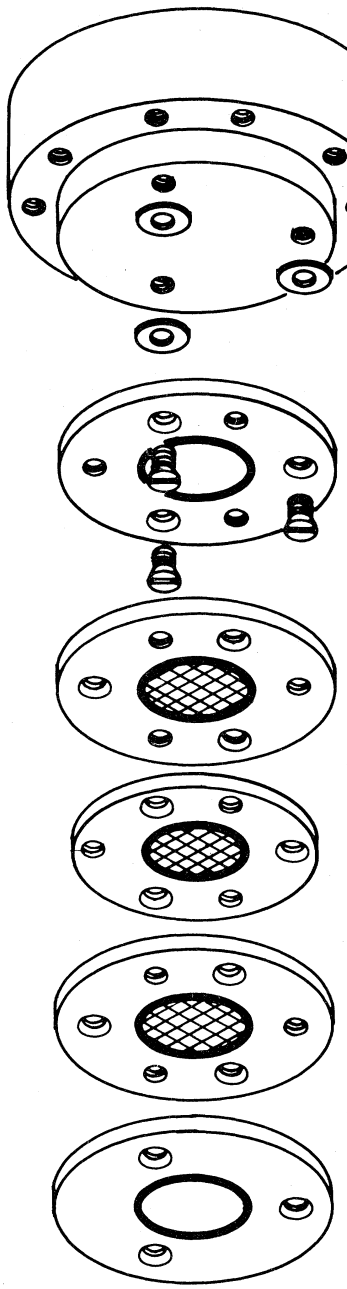

FIG. 1. Top half of the sample-cell body and the five (detached) parallel capacitor plates. Each plate has an active center set in a annular, electrically grounded guard ring. The stainless-steel screens for the three inner plates, shown as cross-hatched lines, are used to speed up hydrostatic equilibrium. When assembled, the total height of the five plates is 1.2 cm and outer diameter of each guard ring is about 3 cm. The plates are separated by thin washers which are 0.0076 cm thick. Other details are given in the text.

contain uncertainties that are almost a factor of 2 larger than those found for $N_2$ and Ne. Since the results for HD do not add materially to our major conclusions, they are not presented here.[36] In order to keep this paper coherent in theme and reasonable in length, our results on the coexistence-curve diameter of $N_2$ and Ne will be presented in a separate paper.

The remainder of this paper consists of three main sections. In Sec. II we discuss the cryostat, the sample cell, the low-temperature needle valve, and the measurement of temperature and density with the thermometer and capacitance bridges. In Sec. III we begin with a discussion on the special considerations and precautions taken with regard to the effect of gravitational rounding, temperature gradient, and the correct choice of $T_c$. Results in different temperature ranges and along different thermodynamic paths are then presented systematically. In Sec. IV concluding remarks and comparison between our values for the leading and correction exponents and the amplitude ratios with the theoretically predicted values are made.

## II. EXPERIMENTAL APPARATUS AND PROCEDURES

The details of the cryostat, capacitance bridge (for density determination), resistance bridge (for temperature regulation and measurement), needle valve used to seal the sample cell, and the "five-plate" sample cell used in this experiment, are described below. All of the equipment, except the five-plate sample cell, has already been described in previous publications.[37,38] The sample cell used in those earlier experiments to search for an anomaly in the dielectric constant near the critical point is used as a reference capacitor in this experiment.

### A. Cryostat

The cryostat is suspended from a vibrationally isolated top plate. It fits inside a double-jacket Dewar. For the Ne experiment the inner volume of the Dewar is filled with liquid helium, and the outer with liquid nitrogen. For the $N_2$ experiment both volumes are filled with liquid nitrogen. Retransfer of liquid helium is required every 5 d. The liquid-nitrogen bath lasts 14 d.

The outermost heat shield is suspended from the top plate by stainless-steel tubing and is surrounded by the cryogenic fluid. The outermost heat shield, referred to as the outer vacuum can (OVC), allows evacuation of the entire region around the sample cell and reference cell. Suspended inside the OVC is a second shield or jacket ($J_1$). Its temperature is intermediate between that of the OVC (at 4.2 or 77 K) and the jacket $J_2$ that is closest to the cells. The temperature of $J_2$ ($T_{J_2}$) is controlled by a carbon-resistor thermometer mounted on $J_2$ and is part of the servoheater circuit used for its temperature control. A three-lead measurement scheme eliminates lead resistance. All electrical wiring connecting the cells to the equipment at room temperature passes through the top plate, inside stainless-steel tubing, through the top of the OVC, through $J_1$, and through $J_2$ to the sample cell and reference cell. The wires are thermally anchored at each shield to control and reduce the amount of heat that reaches the cells through the wires.

### B. Sample cell and needle valve

In our cryostat the sample cell and the reference cell (lower) are attached one on top of the other. Both cells are made entirely of oxygen-free high-conductivity copper (OFHC). The five-plate sample cell is a stack of five parallel plates forming four capacitors (Fig. 1). It is actually two halves sealed together with an indium *O*-ring. Suspended from the top half are the five plates. Each plate has an active center electrode set in a guard ring. The guard ring is held to the active plate and electrically isolated by epoxy. Plate 1 is attached to the top half of the cell by three brass (2-56 type) screws. On each screw, identical copper washers leave a 0.0076-cm gap between plate 1 and the top of the cell. Plate 2 is independently suspended from plate 1 in the same way with three screws and washers as spacers. When the top half with all five plates in place is sealed together with the bottom half there is a 0.0076-cm gap between plate 1 and the top half, between each plate, and between plate 5 and the lower half of the cell. Therefore, when filled to the critical density, the position of the meniscus should be close to the geometric center of the cell.

The thicknesses of plates 1–5 are 0.257, 0.241, 0.165, 0.231, and 0.259 cm, respectively. The "thinness" of these plates and the gaps between these plates is chosen to minimize gravitational-rounding effects. The diameter of the electrode of plate 3 is 1.52 cm. The diameters of the electrodes of plates 2 and 4 are 1.65 cm. The diameters of the electrodes of plates 1 and 5 are 1.78 cm. This design minimizes the effect of stray electric field, since in our capacitance measurements the smaller of the two plates forming a capacitor is always close to zero potential and the guard rings are grounded.

The outer diameter of the annular guard ring around plate 3 is smaller (2.90 cm) than that of the guard rings around the other four plates (3.15 cm). This way the majority of volume available to the fluid is in the center of the cell, minimizing the effect of any movement of the meniscus below $T_c$.

To decrease the time required to establish hydrostatic equilibrium, plates 2–4 have many holes drilled through the active part. A stainless-steel screen (0.013 cm thick, perforated with 0.013-cm-diam holes) is soldered onto both sides of the plates. The screen purchased from Buckbee-Mears Company of St. Paul, Minnesota has a transparency of 28%. This configuration allows fluid to move through the plates instead of around them. The effective gap between the plates, because of these holes, are expected to be considerably wider than the nominal 0.0076-cm value. The total volume available to the fluid in the five-plate cell is 2.5 $cm^3$

The fluid is sealed in the sample cell with a needle valve[37] that is actuated externally. It is connected to the cell by 8.5 cm of stainless-steel capillary tubing (0.041 cm o.d. and 0.020 cm i.d.). The volume of this connecting capillary is further reduced by our stuffing it with a 0.013-cm-diam Evan-Ohm wire. The total volume of the needle valve and capillary is less than 0.1% of the cell volume. The temperature of the needle valve is regulated above $T_c$ at $t \cong +1\times10^{-2}$ using a servoheater system identical to the one controlling the temperature of $J_2$. This keeps a small but constant amount of fluid in the valve and connecting capillary.

The sample cell is filled by passing the nitrogen gas (99.999% pure through a zeolite trap submerged in a liquid-acetone bath at −30 °C. For Ne (99.998% pure) the zeolite trap is submerged in liquid nitrogen.

### C. Resistance bridges and temperature determination

A platinum-resistance thermometer ($R_{\mathrm{Pt,high}}$) is soldered onto the sample cell. A second platinum thermometer ($R_{\mathrm{Pt,low}}$) is soldered onto the reference cell. Also, a standard resistor ($R_{\mathrm{st,high}}$) is noninductively wound onto the sample cell and another ($R_{\mathrm{st,low}}$) is wound onto the reference cell. Our standard resistors are made of Evan-Ohm wire that has a negligible temperature coefficient of resistivity. In two separate bridge circuits we measure two resistance ratios defined by $\mathscr{R}_{\mathrm{high}}=R_{\mathrm{Pt,high}}/R_{\mathrm{st,high}}$ and $\mathscr{R}_{\mathrm{low}}=R_{\mathrm{Pt,low}}/R_{\mathrm{st,low}}$ in the Ne experiment. (For the $N_2$ experiment the ratio measured is $R_{\mathrm{st}}/R_{\mathrm{Pt}}$.) The measurement of each $\mathscr{R}$ is a "4" lead ac measurement that eliminates lead resistance.[37] The $\mathscr{R}_{\mathrm{low}}$ circuit is used to control the temperature via a feedback loop. The $\mathscr{R}_{\mathrm{high}}$ circuit is used to measure the temperature.

The thermometer on the reference (lower) cell is calibrated from 90 to 505 K by the manufacturer (Minco Corporation, Minneapolis Minn.). The calibration is traceable to the National Bureau of Standards. Below 90 K we use the International Practical Temperature Scale of 1968 (IPTS-68).[39] We estimate the absolute accuracy of our temperature scale to be ±10 mK above 90 K and ±25 mK below 90 K. In the course of the experiment the stability in $\mathscr{R}_{\mathrm{high}}$ is better than $\pm1\times10^{-7}$ for many hours, which translates to temperature stability of ±30 μK corresponding to $\pm2\times10^{-7}$ and $\pm6\times10^{-7}$ in reduced temperature for $N_2$ and Ne, respectively.

### D. Capacitance bridge and density determination

The dielectric constant is measured with a capacitance bridge setup similar to that used by Chan *et al.*[40] This bridge measures a ratio

$$\mathscr{C}=C_{\mathrm{sample}}(C_{\mathrm{sample}}+C_{\mathrm{ref}})^{-1}\,. \tag{8}$$

In our experiment, at each temperature at least four different ratios are measured by forming different combinations of the capacitors in the five-plate cell and the reference cell. Our labeling convention is

$$\mathscr{C}(12,\mathrm{ref})=C_{12}(C_{12}+C_{\mathrm{ref}})^{-1} \tag{9}$$

where $C_{12}$ is the capacitor formed by plates 1 and 2 of the five-plate cell, and $C_{\mathrm{ref}}$ is the reference capacitor. Similarly, $\mathscr{C}(12,45)$ and $\mathscr{C}(23,34)$ measure ratios $C_{12}(C_{12}+C_{45})^{-1}$ and $C_{23}(C_{23}+C_{34})^{-1}$, respectively. The bridge is operated at 12 $V$ rms and at a frequency of 1041 Hz. Changing the frequency and excitation voltage of the bridge causes no measurable change in our density determination. All electrical leads are coaxial to minimize noise pickup. For all $\mathscr{C}$'s far from the critical point the uncertainty in any ratio is approximately $5\times10^{-8}$. Near

the critical point, large density fluctuations make the uncertainty as large as $5\times10^{-6}$.

Dielectric constant values at the four different heights in our experiment are obtained from the capacitance ratios. The dielectric constant is converted to reduced density by using the Clausius-Mossotti equation[41]

$$\frac{\rho}{\rho_c}=\frac{(\epsilon-1)/(\epsilon+2)}{(\epsilon_c-1)/(\epsilon_c+2)}\ . \tag{10}$$

In general, there are regular corrections to this relationship, however, the corrections for $N_2$ are extremely small[42] (less than 0.05%) over the entire range of this experiment. The law of corresponding states implies comparable corrections for Ne. Since we are interested primarily in density differences, small regular corrections to the Clausius-Mossotti equation are of no consequence. The values of the dielectric constant at the critical points of $N_2$ and Ne that we used are $\epsilon_c=1.155$ (Ref. 35) and 1.0725.[37] The dielectric constant between plates 1 and 2, $\epsilon_1$, is obtained from $\mathscr{C}_S(21,\text{ref})$

$$\epsilon_1=\frac{\mathscr{C}_E(12,\text{ref})^{-1}-1}{\mathscr{C}_S(12,\text{ref})^{-1}-1}\ , \tag{11}$$

where $\mathscr{C}_S$ is the capacitance ratio with the sample and $\mathscr{C}_E$ is the ratio with the gap empty. An identical relation yields $\epsilon_2$ from $\mathscr{C}_S(23,\text{ref})$. $\mathscr{C}(12,45)$ and $\mathscr{C}(23,34)$ measure the ratio $\epsilon_1/\epsilon_4$ and $\epsilon_2/\epsilon_3$, respectively. Typically, $\epsilon_1$ and $\epsilon_2$ are obtained from $\mathscr{C}(12,\text{ref})$ and $\mathscr{C}(23,\text{ref})$ and are used to solve for $\epsilon_3$ and $\epsilon_4$ from $\mathscr{C}(23,34)$ and $\mathscr{C}(12,45)$. The highest temperature at which data is gathered in any run is about $t=4\times10^{-2}$. For $t>1\times10^{-2}$ the $\mathscr{C}$'s are well represented by linear functions of temperature. Here $\chi_T^+$ is so small that changes in density become unresolvable. The linear behavior is due to a combined pressure and temperature deformation of the plates themselves. Data in this range (typically 6—10 points) are fitted to a straight line to obtain initial estimates for the $\mathscr{C}_E$'s. However, these cannot be exactly correct, because if the $\mathscr{C}_S$'s equal the $\mathscr{C}_E$'s at a particular temperature, then the density difference would be identically zero, a physically unreasonable relationship. The actual baselines are straight lines as close as possible to the initial estimates and satisfying the following physical requirements: Both $(\rho_4-\rho_1)/2\rho_c$ and $(\rho_3-\rho_2)/2\rho_c$ must approach zero without becoming negative at high temperatures, and the average density as measured by $(\rho_4+\rho_1)/2$ and $(\rho_3+\rho_2)/2$ must be identical at all temperatures outside the gravity-rounded region; the measurements of $\rho_4$, $\rho_3$, $\rho_2$, and $\rho_1$ are properly scaled to the height differences for $t\gtrsim3\times10^{-3}$. The combined uncertainties in the $\mathscr{C}_E$'s translate to an uncertainty in $(\rho_4-\rho_1)/2\rho_c$ and $(\rho_3-\rho_2)/2\rho_c$ of about $2\times10^{-5}$. The percent uncertainty diminishes as $\Delta\rho^*$ increases. At $t=5\times10^{-3}$ the uncertainty in the $\mathscr{C}_E$'s introduces a 3% uncertainty in $(\rho_4-\rho_1)/2\rho_c$. At $t=1\times10^{-3}$ the uncertainty in $(\rho_4-\rho_1)/2\rho_c$ is approximately 1%. By $t=1\times10^{-4}$, the uncertainty in $(\rho_4-\rho_1)/2\rho_c$, due to the uncertainty in the $\mathscr{C}_E$'s, is less than 0.2%. The percent uncertainty in $(\rho_3-\rho_2)/2\rho_c$, due to the uncertainty in the $\mathscr{C}_E$'s, is a factor of 3 larger than the percent uncertainty in $(\rho_4-\rho_1)/2\rho_c$ at any temperature above $T_c$ because $\Delta h$ is 3 times smaller. For $1\times10^{-4}>t>-1\times10^{-4}$, the primary source of uncertainty in $\Delta\rho^*$ is the fluctuations in the density near the critical point. the uncertainty is about 0.2% at $|t|=1\times10^{-4}$ and reaches 1% for $|t|<1\times10^{-5}$. Farther below $T_c$, where the fluctuations in density become small and the density difference becomes larger, the uncertainty in $(\rho_4-\rho_1)/2\rho_c$ and $(\rho_3-\rho_2)/2\rho_c$ becomes approximately 0.02%. Based upon the above-mentioned uncertainties, we adopt a criterion for allowable scatter in the residual to be (1) 0.1% for the order-parameter analysis, (2) 2% for the cubic model analysis, and (3) 5% for the one-phase compressibility analysis.

## III. DATA ANALYSIS

For data analysis we adopt the following values for the critical constants for $N_2$ (Ref. 35) and Ne.[37] The critical pressures in dyn/cm$^2$ for $N_2$ and Ne, respectively, are $P_c=3.398\times10^7$ and $2.72\times10^7$, and the critical densities in g/cm$^3$ are $\rho_c=0.314$ and 0.484. The value of $g$, the gravitational constant, is assumed to be 981 cm/s$^2$.

Three experimental complications exist for pure fluids near the critical point, which must be cautiously considered in data analysis. They are (1) gravitational rounding, (2) elimination of temperature gradients, and (3) correct determination of $T_c$. We consider them in order.

### A. Gravitational rounding

In the earth's gravitational field there is a contribution to the chemical potential that is proportional to the height $z$ above the height $z_0$ where $\rho=\rho_c$ in the fluid. The $\rho_L$ and $\rho_V$ of Eq. (1) are found strictly at the meniscus separating the two phases. However, measurements are typically at a finite height below and above the meniscus, and are an average over a finite measuring height. As $t$ approaches zero and $\chi_T$ diverges, the measured densities deviate further from the true coexisting densities. An independent determination of this gravity effect is necessary to know which data can be fitted to Eq. (5). Likewise, in our measurement of $\chi_T^+$, we assume $\partial\rho/\partial\mu\cong\Delta\rho/g\Delta h$ where $\Delta h$ is the difference in height between the two density measurements. Very near $T_c$ the density gradient changes so sharply with height that this approximation fails.[34,35] The effect of gravity cannot be eliminated unless the experiment is performed in an extremely-low-gravity environment. However, with the information obtained from our five-plate sample cell, we are able to determine over what temperature range our measurements are significantly affected by gravity. Data which deviate from a specific thermodynamic path due to the effect of gravity are said to be in the "gravitationally rounded" region. Data in the gravitationally rounded region are excluded from power-law analyses, and are analyzed using the restricted cubic model equation of state which is discussed below.

A further gravitational effect is the error in a single density measurement that results from averaging over a finite height. This is of secondary importance in our experiment. It causes a 1% error for $|t|<1\times10^{-5}$ and much smaller error farther from $T_c$. Details of this type of error have been discussed elsewhere.[34,35]

### B. Suppression of thermal gradients

A second subtle difficulty in our experiment is the effect of a temperature gradient. If present along the cell, a temperature gradient contributes to the chemical potential an amount proportional to $(\partial P/\partial T)(\partial T/\partial z)$. For $N_2$, $(\partial P/\partial T)\rho_c = 1.715\times 10^6$ dyn/cm$^2$/K.[43] Therefore, a temperature gradient of 0.2 mK/cm from top to bottom will make a contribution to the chemical potential comparable to that from gravity. For Ne the number is approximately 0.15 mK/cm.[35] The presence of gradients can severely complicate the analysis, rendering Eq. (6) incomplete and destroying the simple connection between the parametric model parameters and the power-law amplitudes. Independent information on temperature gradients is essential to validate high-precision measurements.

In the assembly of the cryostat, we had this problem in mind. Heat leaks from the sample cell and reference cell to $J_2$ are carefully installed to minimize any temperature gradients along the cells. The top of the five-plate sample cell is suspended from $J_2$ by the three stainless-steel thin-wall tubes 0.318 cm in diameter with a 0.025-cm wall thickness. The bottom of the lower cell and $J_2$ are connected by three (identical but flattened) stainless-steel tubes. This configuration provides almost identical thermal links from $J_2$ to the top and to the bottom of the two stacked cells. The electrical leads and fill capillaries for each cell have nearly negligible conductivity compared to the tubing. In order to compensate for any uneven heat leak to $J_2$, the heating configuration on the cells has two heater wires in parallel; one is wrapped around the top of the top cell and the other is wrapped around the bottom of the lower cell. Externally, a resistance decade box is attached in series with one of the heater wires. Use of this external resistance enables us to adjust the proportion of heat to the top and bottom cells, giving us total control over temperature gradients.

The greater the total amount of heat that is applied directly to the sample cell and reference cell, the greater the possibility of a temperature gradient along the cells. The amount of heat needed directly on the cells can be decreased by increasing the temperature of $J_2$. However, increasing $T_{J_2}$ reduces the possible range of data acquisition because the lowest possible reduced temperature of the sample cell is the reduced temperature of $J_2$. The amount of heat required to maintain the temperature of the cells are 5 mW for $N_2$ and 4 mW for Ne. Given the thermal conductivity of OFHC (which has its maximum value around 30 K), the total amount of heat going to the sample cell, and the dimensions of the cells, we calculate the maximum possible temperature gradient near $T = T_c$ to be 15 $\mu$K/cm for $N_2$ and 3 $\mu$K/cm for Ne. The calculation assumes a configuration of heating that is mismatched from the thermal link to $J_2$ by 5%. The 5% value is based upon tests we have performed by systematically adjusting the heat distribution on the cells and the temperature of $J_2$. It follows that our density profile at $T_c$ is different from the density profile due to gravity alone by no more than 7% for $N_2$ and 2% for Ne. The uncertainty in our determination of $D_0$ (discussed below) is larger than this, and thus the uncertainty in the temperature gradient is not the limiting factor in our determination of $D_0$.

There is additional evidence that we have no significant temperature gradient in our measurements. First, we find excellent agreement between the results as determined by power-law analysis and by cubic model analysis (discussed below). Second, the values of $\Gamma_0^+$, as determined by density measurements in different capacitor gaps, approach each other as the heating configuration approaches the one that we determined to be optimum.

### C. Determination of the critical temperature

Standard procedure for analyzing data in the critical region is to let the amplitudes, exponents, and $T_c$ be free parameters in a least-squares-fitting routine. The results for the exponents and amplitudes are particularly sensitive to the choice of $T_c$. Experience has shown us that it is possible to obtain good-quality fits to experimental data with incorrect values for the free parameters. This can happen by including data that is not on the appropriate thermodynamic path (e.g., in the gravity-rounded region) or by not including correction-to-scaling terms for data outside the asymptotic critical region. With our five-plate sample cell we know when our order-parameter and compressibility measurements deviate from their appropriate thermodynamic paths, so $T_c$ as a free parameter is not shifted by erroneously including data in the gravity-rounded region. Furthermore, most experiments collect data on only one thermodynamic path. With our capacitance technique, we make measurements on both the coexistence curve and the critical isochore. To restrict the values of $T_c$ as a free parameter, we should, ideally, analyze data above and below $T_c$ simultaneously. However, this is technically difficult because the precision of our density-difference determinations below and above $T_c$ are different by as much as 2 orders of magnitude. We allow $T_c$ to be a free parameter for analysis of the order parameter on the coexistence curve [Eq. (5)], for analysis of the compressibility above $T_c$ [Eq. (6)], and for analysis near $T_c$ using the restricted cubic model. All of this analysis, to be discussed below, is summarized in Tables I–II. For the three types of analysis we find that $T_c$ as a free parameter is the same to within 0.2 mK for $N_2$ and 0.3 mK for Ne. The statistical uncertainty in $T_c$ for each type of analysis is considerably (at least by a factor of 3) smaller than 0.2 mK.

### D. Order parameter

Figure 2 shows plots of $\Delta\rho^*$ versus reduced temperature for Ne. Figure 3 shows the region near $T_c$ in more detail for $N_2$. The squares are $\rho_4$ and $\rho_1$; the circles are $\rho_3$ and $\rho_2$. This plot tells us *a priori* which data must be excluded from a fit to Eq. (5). Where the two sets deviate from each other indicates when each measurement deviates from the true coexistence curve. For $N_2$ and Ne, at a reduced temperature below $T_c$ of $|t| \cong 1.5\times 10^{-3}$, we observe that $\rho_4$ and $\rho_3$ differ by about 0.1%. Therefore, a power-law analysis of $(\rho_4-\rho_1)/2\rho_c$, which is accurate to 0.1%, should be limited to data in the region $|t| > 1.5\times 10^{-3}$. Since $\rho_1$ and $\rho_4$ are further from the meniscus and $\chi_T$ scales as $(\Delta h)^\gamma$, the rounded region is larger by a factor of about 4 in reduced temperature for

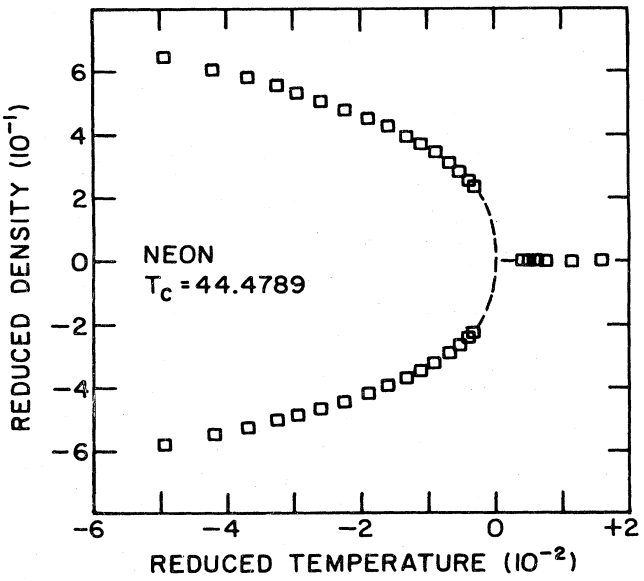


FIG. 2. Coexistence curve of Ne in reduced units. There is a large number of data points near $T=T_c$; for clarity they are represented by dashed lines.

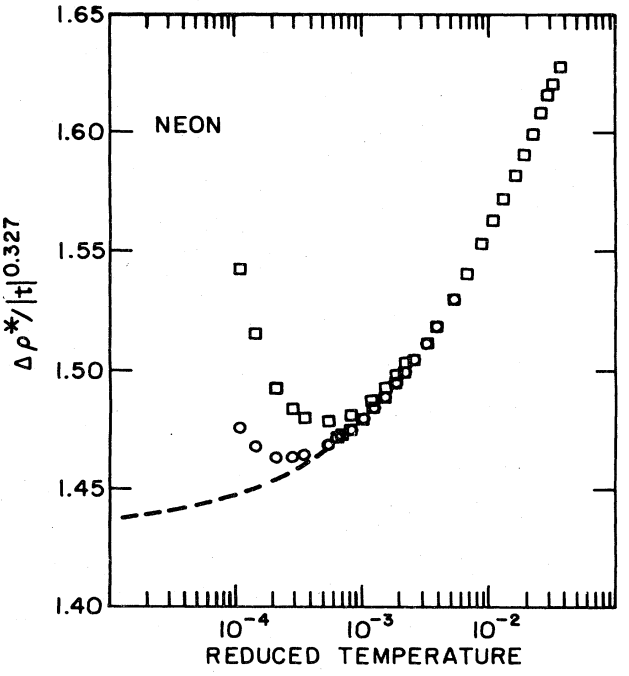


FIG. 4. Plot of $\Delta\rho^*/|t|^{0.327}$ for Ne. The squares represent data from the two outer capacitor gaps and the circles represent data from the two inner capacitor gaps. Deviation from a horizontal line at large $|t|$ indicates the need for correction-to-scaling terms. The dashed line comes from a power-law analysis with all parameters except $\Delta$ floating (lines 13 and 18 of Table I). Gravitational rounding becomes important for the outer data set inside $|t|=1\times10^{-3}$ and the inner data set inside $|t|=4\times10^{-4}$.

them than for $\rho_2$ and $\rho_3$. Therefore, our order-parameter analysis of $(\rho_4-\rho_1)/2\rho_c$ stops at $|t|=1.5\times10^{-3}$, for both $N_2$ and Ne, and the analysis of $(\rho_3-\rho_2)/2\rho_c$ stops at $|t|=4\times10^{-4}$. A plot of $\Delta\rho^*/|t|^{\beta}$ vs $t$ (Fig. 4) is a sensitive way to examine the power-law behavior; this plot also shows the need for corrections to the simple power law for large $|t|$ and the effect of gravity for small $|t|$. The dashed line shows the continuation of our fit into the gravity-rounded region. Asymptotically, it approaches the value of $B_0$. The squares are $(\rho_4-\rho_1)/2\rho_c$; the circles are $(\rho_3-\rho_2)/2\rho_c$. If a simple power law were sufficient, such a plot would be a horizontal line outside the gravity-rounded region. For $|t|>5.0\times10^{-4}$ the data are not on a horizontal line, indicating the need for correction terms. The upward curvature in the region $|t|<5\times10^{-4}$ is due to gravity effects; the measurement of $\Delta\rho^*$ is no longer the order parameter since, at $T$ near $T_c$, $\Delta\rho^*$ is larger than $\rho_L-\rho_V$ at the meniscus. Figure 4 also shows, as expected, that the gravitational effect appears further from $T_c$ for the order parameter as measured by the outermost capacitor gaps. Inside the appropriate temperature range $(\rho_4-\rho_1)/2\rho_c$ and $(\rho_3-\rho_2)/2\rho_c$ are fit to Eq. (5) separately. A nonlinear least-squares-fitting routine adopted from Bevington[44] is used. The results of the analysis are summarized in Table I along with the range of analysis and the number of data points used. Four data sets as measured by the two outer capacitor gaps and the two inner capacitor gaps of the two fluids are analyzed in six different ways: (1) all five parameters in Eq. (5) ($T_c$, $\beta$, $B_0$, $B_1$, and $B_2$) are left free so as to minimize the $\chi^2$, (2) $\beta$ is fixed at 0.325, (3) $T_c$ is held fixed at the value determined by cubic model analysis (discussed below), (4) $T_c$ and $\beta$ are held fixed, (5) assuming only one correction term ($B_2=0$) with $T_c$ fixed at the "optimum" value, and (6) $B_2=0$, but $T_c$ free (for $N_2$ only). The correction exponent is fixed at $\Delta=0.5$ for all these fits. Fixed parameters are enclosed in parentheses in Table I.

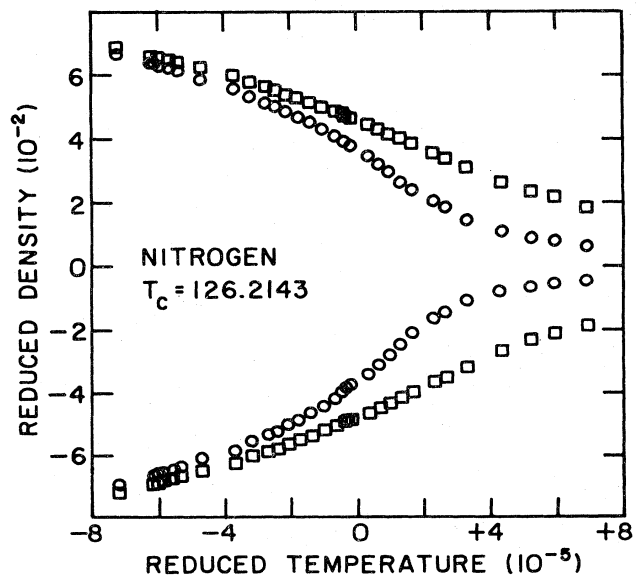


FIG. 3. Reduced density of $N_2$ vs reduced temperature inside $|t|=8\times10^{-5}$ at four heights as determined by our five parallel stacked capacitor plates.

TABLE I. Analysis of the order-parameter data to the form $\Delta\rho^* = B_0 |t|^{\beta}(1 + B_1 |t|^{0.5} + B_2 |t|)$. Fixed parameters are shown in parentheses.

| | $T_c$ | $\beta$ | $B_0$ | $B_1$ | $B_2$ | $\chi^2$ |
|---|---|---|---|---|---|---|
| $N_2$ | $(\rho_4-\rho_1)/2\rho_c$ | $-2\times10^{-2} < t < -1.5\times10^{-3}$ | | | 31 points | |
| 1 | 126.2142 | 0.3253 | 1.478 | 1.06 | −2.08 | 1.55 |
| 2 | 126.2137 | (0.3250) | 1.472 | 1.08 | −2.16 | 2.78 |
| 3 | (126.2143) | 0.3285 | 1.516 | 0.90 | −1.70 | 1.45 |
| 4 | (126.2143) | (0.3250) | 1.482 | 0.96 | −1.58 | 20.21 |
| 5 | (126.2143) | 0.3261 | 1.512 | 0.63 | (0) | 200 |
| 6 | (126.2018) | 0.3236 | 1.510 | 0.57 | (0) | 50 |
| $N_2$ | $(\rho_3-\rho_2)/2\rho_c$ | $-6\times10^{-3} < t < -4\times10^{-4}$ | | | 33 points | |
| 7 | 126.2141 | 0.3262 | 1.483 | 1.04 | −2.31 | 1.00 |
| 8 | 126.2136 | (0.3250) | 1.475 | 1.00 | −1.79 | 1.75 |
| 9 | (126.2143) | 0.3262 | 1.482 | 1.07 | −2.50 | 0.88 |
| 10 | (126.2143) | (0.3250) | 1.473 | 1.00 | −1.51 | 6.67 |
| 11 | (126.2143) | 0.3254 | 1.486 | 0.80 | (0) | 6.70 |
| 12 | 126.2113 | 0.3252 | 1.496 | 0.70 | (0) | 1.0 |
| Ne | $(\rho_4-\rho_1)/2\rho_c$ | $-4\times10^{-2} < t < -1.5\times10^{-3}$ | | | 21 points | |
| 13 | 44.4786 | 0.3272 | 1.436 | 0.99 | −1.58 | 1.00 |
| 14 | 44.4781 | (0.3250) | 1.420 | 1.00 | −1.51 | 1.10 |
| 15 | (44.4789) | 0.3276 | 1.437 | 1.01 | −1.66 | 1.00 |
| 16 | (44.4789) | (0.3250) | 1.419 | 1.00 | −1.48 | 3.01 |
| 17 | (44.4789) | 0.3270 | 1.452 | 0.69 | (0) | 55 |
| Ne | $(\rho_3-\rho_2)/2\rho_c$ | $-6\times10^{-3} < t < -4\times10^{-4}$ | | | 18 points | |
| 18 | 44.4788 | 0.3275 | 1.432 | 1.09 | −2.16 | 1.08 |
| 19 | 44.4784 | (0.3250) | 1.415 | 1.01 | −1.07 | 1.83 |
| 20 | (44.4789) | 0.3274 | 1.427 | 1.17 | −2.72 | 1.00 |
| 21 | (44.4789) | (0.3250) | 1.411 | 1.00 | −0.4 | 9.17 |
| 22 | (44.4789) | 0.3262 | 1.426 | 0.90 | (0) | 1.1 |

We shall first comment on the fits that include the second correction term. For $N_2$ we find the critical parameters as follows: $T_c = (126.2143 \pm 0.0002)$ K, $\beta = 0.327 \pm 0.002$, $B_0 = 1.479 \pm 0.006$, $B_1 = 1.02 \pm 0.06$, and $B_2 = -2.0 \pm 0.5$; for Ne we find $T_c = (44.4789 \pm 0.0003)$ K, $\beta = 0.327 \pm 0.002$, $B_0 = 1.425 \pm 0.010$, $B_1 = 1.02 \pm 0.07$, and $B_2 = -1.6 \pm 0.6$. The value we found for $T_c$ by allowing all parameters to be free is in excellent agreement (within 0.2 mK for $N_2$ and 0.3 mK for Ne) with that found in a cubic model analysis of data near $T_c$ and power-law analysis of one-phase isothermal compressibility. This agreement is reflected in the quoted uncertainties of the critical temperatures. These uncertainties do not enclose the $T_c$ values with $\beta$ fixed at 0.325. Indeed, Table I shows, by the $\chi^2$ values, that our data prefer a value for $\beta$ that is higher than 0.325, for instance, 0.327. Since the cubic model analysis is most sensitive to the choice of $T_c$, the cubic model value is considered to be the canonical value. The uncertainty in $T_c$ is relative in nature in that the temperature scale, as discussed above, is reliable to $\pm 10$ mK for $T > 90$ K and $\pm 25$ mK for $T < 90$ K. It should be noted that consistent values for $\beta$ as well as $B_0$ and $B_1$ are found by using different methods of analysis on the "outer" $(\rho_4-\rho_2)/2\rho_c$ and "inner" $(\rho_3-\rho_2)/2\rho_c$ data sets; the uncertainty quoted for $\beta$ reflects the total variations, and the uncertainty quoted for the amplitudes enclose six of the eight values obtained from our four fits on the two data sets. The uncertainty quoted here is at least a factor of 3–4 larger than the statistical uncertainty. The statistical uncertainty does not take into account the correlations between the free parameters.

Since the number of data points and the estimated random error are different for each data set, the $\chi^2$ value shown in Table I and in subsequent tables should only be used to estimate the relative "goodness" of the various fits applied to a single data set. In addition to the $\chi^2$ value, the goodness of a fit can be evaluated by inspection of the percentage residual, that is the percentage difference between the fitted and the actual measured value of the fit, as a function of reduced temperature. Such a plot is shown in Fig. 5. For the sake of brevity, only the fits, one each for $N_2$ and Ne, allowing all parameters except $\Delta$ free, are shown. The residual percentages from outer and inner data sets are combined in these plots. In the entire temperature range $2\times10^{-2} > |t| > 4\times10^{-4}$, the residuals of the $N_2$ data lie inside 0.03% and show no noticeable systematic trend. The Ne residuals, in the range $4\times10^{-2} > |t| > 4\times10^{-4}$, also show no systematic trend and lie inside 0.15%. We do not know exactly why the scatter in Ne in this region and other regions is worse than that in $N_2$; it is probably due to the fact the smaller dielectric constant value of Ne reduces the sensitivity of

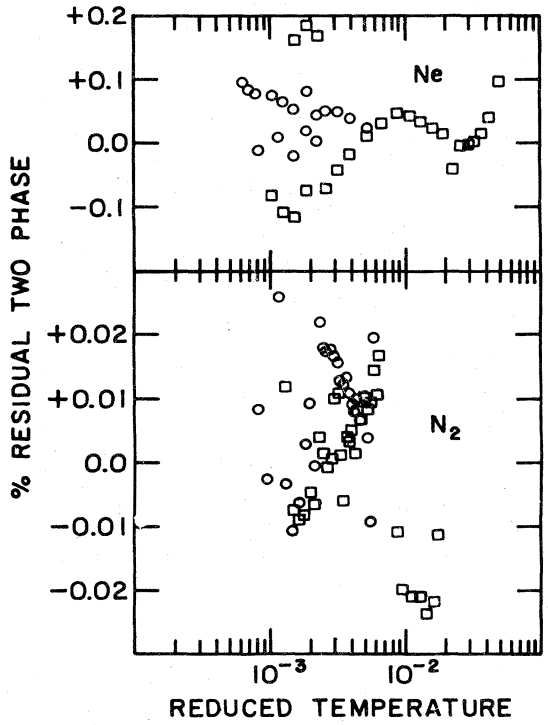


FIG. 5. Percentage residual of the power-law fit of the order parameter of $N_2$ and Ne to the form $\Delta\rho^* = B_0|t|^{\beta}(1+B_1|t|^{\Delta}+B_2|t|^{2\Delta})$. All parameters, except $\Delta$ (equal to 0.5), are floating in the fit (lines 1 , 7, 13, and 18 of Table I). Squares and circles are data from, respectively, the outer and inner capacitor gaps.

our capacitance technique, and that we were forced, by the 5-d helium-bath life, to gather Ne data at a quicker pace. In any case, the residuals shown in Fig. 5 compare very favorably with all published data near the critical point. The residual plots for other fits exhibit the expected correlation with the $\chi^2$ values.

It should be pointed out that the physical significance of the amplitudes $B_2$ is not clear.[10,11,17,18] However, the $\chi^2$ value for fits that exclude the $B_2$ terms shown in Table I indicate that such a term is clearly needed for the outer data sets and less important for the inner data sets. This is the case since the temperature range of the outer data sets are farther from $T_c$, namely $3\times10^{-2} > |t| > 1.5\times10^{-3}$ for the outer data sets, versus $6\times10^{-3} > |t| > 4\times10^{-4}$ for the inner. The second correction term is expected to be more important at large $|t|$. Below a certain minimum temperature, we find that $\rho_2$ becomes suddenly nearly identical to $\rho_3$, indicating that the gap between plates 2 and 3 due to the capillary rise effect[45,46] is wetted by the liquid. Since the liquid-vapor surface tension vanishes near the critical point with a power law, this effect is present only for large $|t|$. This prevents us from obtaining useful data on $(\rho_3-\rho_2)/2\rho_c$ for $|t| > 6\times10^{-3}$. For the outer data sets, the $\chi^2$ value we found by excluding the second correction term is about a factor of 50—100 larger than that found by excluding the $B_2$ term. This is the case with either $T_c$ fixed at the cubic model value or with $T_c$ left as a free parameter (shown for $N_2$ only). The percent residual of these fits show large systematic trends with reduced temperature, at the maximum (worst) value, it is about a factor of 10 larger than those shown in Fig. 5. In spite of these difficulties, the values found for $\beta$ and $B_0$ are in reasonable agreement with those including the $B_2$ term. The value of $B_1$ found here are 30—40 % smaller. For the inner data sets, the exclusion of the second correction term does not cause as much difficulty: The $\chi^2$ value does not increase much. For $N_2$, if all parameters are left free, the new $T_c$ value, although changed, strays away from 126.2143 K by 3 mK as compared to 12 mK for the outer data set. The values we found for $\beta$, $B_0$, and even $B_1$ are in reasonable agreement with the analyses with a $B_2$ term. The values of $B_1$ in these fits are, respectively, 20% (for $N_2$) and 10% smaller than those in fits including $B_2$.

In a recent interferometric experiment on $SF_6$ studying the capillary rise between two closely spaced plates, Moldover and Gammon[46] found an anomalously thick film that intrudes between the interferometric plates and the vapor for $T < T_C$. The thickness was found to be independent of temperature, but the density changes as the bulk liquid.

If a similar wetting liquid layer is present in our vapor capacitance gaps, the thickness is expected to be about 1000 Å, or 0.2% of the 0.0076-cm capacitor gap. A liquid layer of this magnitude may cause a systematic error in our vapor-density determination on the order of 0.2%. This possible systematic error does not alter our results since the uncertainties we found in the leading amplitudes $B_0$ are larger. This effect is not present for data gathered in the one-phase region, including those used for deducing the one-phase compressibility and cubic model parameters. This effect is insignificant in comparison to the observed uncertainties for the two-phase compressibility and critical isotherm data. This effect is important in determining the behavior of the coexistence-curve diameter.[46]

### E. Experimental determination of the correction exponent Δ

In the above-mentioned analysis, the correction exponent was held fixed at $\Delta=0.50$. We have repeated the analysis of the order parameter, using two correction terms with $\Delta$ as a free parameter. The high quality of our data allows us to undertake this type of analysis. The results are summarized in Table II. The temperature range of analysis and the number of data points used here are the same as for the analysis shown in Table I. This table shows that the correction exponent $\Delta$ is $0.51\pm0.03$ for $N_2$ and $0.49\pm0.05$ for Ne. These values are in good agreement with the values predicted by RG and the high-temperature-series—expansion method.[7] The amplitudes $B_0$ and $B_1$, as well as $T_c$ and $\beta$, are not affected by allowing $\Delta$ to be a free parameter. These results also confirm that the leading exponent $\beta$ is slightly larger than the predicted value of 0.325. When $\beta$ is held fixed at 0.325 in the analysis, $\chi^2$ increases noticeably as it did when $\Delta$ is fixed at 0.5.

TABLE II. Analysis of the order-parameter data to the form $\Delta\rho^* = B_0 |t|^{\beta}(1 + B_1 |t|^{\Delta} + B_2 |t|^{2\Delta})$. The exponent $\Delta$ is left floating. Fixed parameters are shown in parentheses.

| | $T_c$ | $\beta$ | $B_0$ | $B_1$ | $B_2$ | $\Delta$ | $\chi^2$ |
|---|---|---|---|---|---|---|---|
| $N_2$ | $(\rho_4-\rho_1)/2\rho_c$ | | $-2\times10^{-2} < t < -1.5\times10^{-3}$ | | | 31 points | |
| 1 | 126.2143 | 0.3262 | 1.485 | 1.08 | −2.32 | 0.500 | 1.00 |
| 2 | (126.2143) | 0.3259 | 1.488 | 1.18 | −2.93 | 0.529 | 1.90 |
| 3 | (126.2143) | (0.3250) | 1.480 | 1.00 | −1.78 | 0.502 | 18.3 |
| $N_2$ | $(\rho_3-\rho_2)/2\rho_c$ | | $-6\times10^{-3} < t < -4\times10^{-4}$ | | | 33 points | |
| 4 | 126.2143 | 0.3274 | 1.497 | 0.91 | −1.71 | 0.486 | 1.00 |
| 5 | (126.2143) | 0.3268 | 1.489 | 1.01 | −2.28 | 0.496 | 1.00 |
| 6 | (126.2143) | (0.3250) | 1.480 | 1.00 | −1.16 | 0.524 | 18.8 |
| Ne | $(\rho_4-\rho_1)/2\rho_c$ | | $-4\times10^{-2} < t < -1.5\times10^{-3}$ | | | 21 points | |
| 7 | 44.4790 | 0.3258 | 1.407 | 0.93 | −1.19 | 0.453 | 1.20 |
| 8 | (44.4789) | 0.3256 | 1.418 | 0.99 | −1.44 | 0.489 | 2.95 |
| 9 | (44.4789) | (0.3250) | 1.420 | 1.00 | −1.49 | 0.503 | 2.90 |
| Ne | $(\rho_3-\rho_2)/2\rho_c$ | | $-6\times10^{-3} < t < -4\times10^{-4}$ | | | 18 points | |
| 10 | 44.4788 | 0.3255 | 1.416 | 0.96 | 0.02 | 0.497 | 1.10 |
| 11 | (44.4789) | 0.3257 | 1.415 | 0.95 | −0.04 | 0.491 | 1.20 |
| 12 | (44.4789) | (0.3250) | 1.420 | 1.00 | 2.88 | 0.548 | 4.45 |

We have also analyzed the $N_2$ and Ne order-parameter data according to Eq. (5) with $T_c$ and $\beta$ fixed at the "optimum" values ($T_c = 126.2143$ K for $N_2$ and 44.4789 K for Ne and $\beta = 0.327$), but with the values of $\Delta$ systematically changed from 0.40 to 0.60. The $\chi^2$ value, as a function of the imposed value of $\Delta$ for one set of $N_2$ data, is shown in Fig. 6. A sharp minimum of $\chi^2$ is found at $\Delta = 0.52$. This is in agreement with the analysis shown above with $\Delta$ as a free parameter. Similar sharp minima of $\chi^2$ are seen for the other sets of data. The minimum $\chi^2$ occurs at $\Delta = 0.48$ for Ne. Our results on $N_2$ and Ne presented here are probably the strongest evidence to date that $\Delta$ is in fact equal to a value near 0.5.

### F. One-phase isothermal compressibility

Figure 7 is a log-log plot of $\chi_T^+$, the one-phase isothermal compressibility versus reduced temperature for $N_2$. The squares represent the compressibility as measured by $\rho_4-\rho_1$; the circles are for $\rho_3-\rho_2$. The reduced temperature at which the two sets begin to deviate from each other gives a rough idea at what temperature the approximation $\partial\rho/\partial\mu \cong \Delta\rho/\Delta\mu$ is faulty, and therefore which data points should be excluded from a fit to Eq. (6). A plot of $\chi_T^+/t^{-\gamma}$ vs $t$, shown with the same temperature scale in Fig. 7, clearly indicates the need for a correction term.

The single-phase analysis of $\chi_T^+$ simultaneously fits both density differences $\rho_4-\rho_1$ and $\rho_3-\rho_2$ to Eq. (6). This is possible because they are both scaled by the appropriate height factor. A second correction term of the form $\Gamma_2^+ t^{2\Delta}$ is not included in any fit because its significance is completely masked in the uncertainty in the density measurement. At $t = 3\times10^{-3}$, the percentage scatter in the density difference is about 2%. If the amplitude of the second correction term is unity, it contributes only

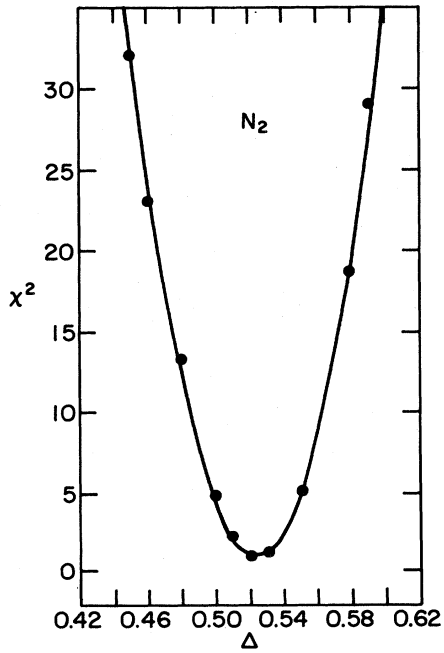


FIG. 6. $N_2$ data from the outer capacitor gaps are fitted to the form $\Delta\rho^* = B_0 |t|^{0.327}(1 + B_1 |t|^{\Delta} + B_2 |t|^{2\Delta})$ with $T_c$ fixed at 126.2143, and with $B_0$, $B_1$, and $B_2$ floating. The $\chi^2$ of the fit as a function of the imposed $\Delta$ is shown in this figure.

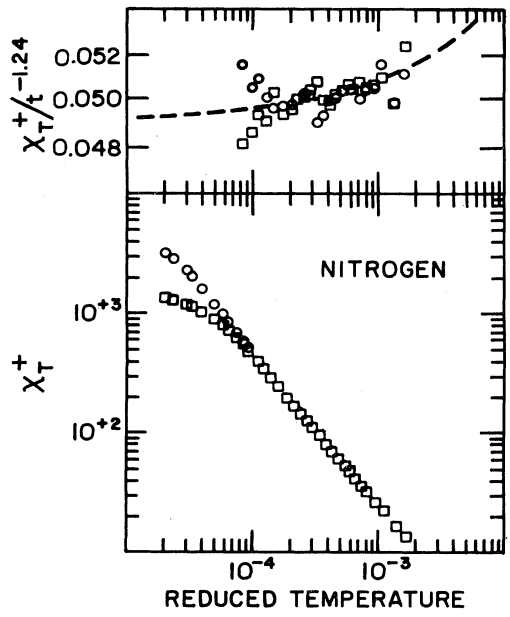


FIG. 7. Lower panel: The one-phase ($T > T_c$) dimensionless isothermal compressibility $\chi_T^+$ as a function of reduced temperature as determined by the outer (squares) and inner (circles) capacitor gaps. The circles coincide with the squares outside $t = 1\times10^{-4}$; they are not shown for the sake of clarity. Upper panel: $\chi_T^+/t^{-1.24}$ as a function of reduced temperature; the upward trend as $t$ is increased indicates the need for correction-to-scaling term. The dashed line results from a power-law fit to the form $\chi_T^+ = \Gamma_0^+ t^{-\gamma}(1+\Gamma_1^+ t^{\Delta})$, with all parameters except $\Delta$ (equal to 0.5) floating (line 1 of Table III).

0.3% at this temperature. Since the analysis extends to a range of about $3\times10^{-3} > t > 7\times10^{-5}$ for $N_2$ and Ne, the second correction-to-scaling term is not justified. For $N_2$ we find $\gamma = 1.233\pm0.01$; for Ne, $\gamma = 1.250\pm0.015$. Table III also shows the results with $\gamma$ fixed at 1.240 as predicted by RG theory. The values of $T_c$ as free parameters are in excellent agreement (within 0.2 mK) with the values obtained from power-law analysis of the order parameter.

For $N_2$ we find $\Gamma_0^+ = 0.048\pm0.001$ and $\Gamma_1^+ = 1.07 \pm 0.06$. For Ne, $\Gamma_0^+ = 0.053\pm0.003$ and $\Gamma_1^+ = 1.15\pm0.15$. The uncertainties quoted enclosed the fitted values by four different methods of analysis.

In Fig. 8 the percentage residual of the fit allowing all parameters except $\Delta$ equal to (0.5) to be free is shown for $N_2$. As discussed above, due to the much smaller density difference, the percentage residual is much larger than that in the two-phase region. Inside $t = 1\times10^{-4}$, systematic deviations in residuals begin to show up between the data from the inner and the outer capacitor gaps. This is probably due to gravitational-rounding effects. When the data inside $t = 1\times10^{-4}$ (eight points) are excluded from the analysis, no noticeable change in the fitted parameters are found. Plots for Ne similar to Figs. 7 and 8 are not shown; they are indeed similar to the $N_2$ plots. The percentage residuals for Ne is again slightly larger than the $N_2$ data.

The one-phase—compressibility data also contains strong evidence that there is no significant temperature gradient. We have repeated the experiment eight times on nitrogen, each time adjusting the distribution of heat from the top and bottom heater to intentionally impose a temperature gradient. We spanned a range as large as possible until the temperature gradient set up turbulence, making it impossible to measure $\chi_T^+$. Near the center of the sample cell the fluid is closer to the critical density and, therefore, is more strongly affected by temperature gradients. When the amount of heat input from the top heater is within 5% of the amount from the bottom heater, we found an identical (to within 1%) value of $\chi_T^+$ according to the two inner capacitor gaps ($\rho_3-\rho_2$), and two outer capacitor gaps ($\rho_4-\rho_1$) in the range $1\times10^{-3} > t > 2\times10^{-4}$. When heat is redistributed within this 5% limit, we also found no measurable effect on the density-versus-height profile even inside the gravity-rounded region. Outside the 5% limit, noticeable effects on $\chi_T^+$ and density profile near $T_c$ are found. Our estimate of the maximum temperature gradient along the cell is based on these studies. The measurements reported here used the optimum distribution of heat from top and bottom.

TABLE III. Analysis of the one-phase dimensionless isothermal compressibility data to the form $\chi_T^+ = \Gamma_0 t^{-\gamma}(1+\Gamma_1 t^{0.5})$. Fixed parameters are shown in parentheses.

| | $T_c$ | $\gamma$ | $\Gamma_0^+$ | $\Gamma_1^+$ | $\chi^2$ |
|---|---|---|---|---|---|
| $N_2$ | | $7\times10^{-5} < t < 1\times10^{-3}$ | | | 45 points |
| 1 | 126.2143 | 1.233 | 0.049 | 1.10 | 1.00 |
| 2 | 126.2141 | (1.240) | 0.047 | 1.06 | 1.19 |
| 3 | (126.2143) | 1.233 | 0.049 | 1.01 | 1.01 |
| 4 | (126.2143) | (1.240) | 0.047 | 1.12 | 1.23 |
| Ne | | $7\times10^{-5} < t < 3\times10^{-3}$ | | | 30 points |
| 5 | 44.4787 | 1.251 | 0.051 | 1.30 | 1.01 |
| 6 | 44.4788 | (1.240) | 0.056 | 1.02 | 1.05 |
| 7 | (44.4789) | 1.250 | 0.051 | 1.10 | 1.36 |
| 8 | (44.4789) | (1.240) | 0.055 | 1.07 | 1.15 |

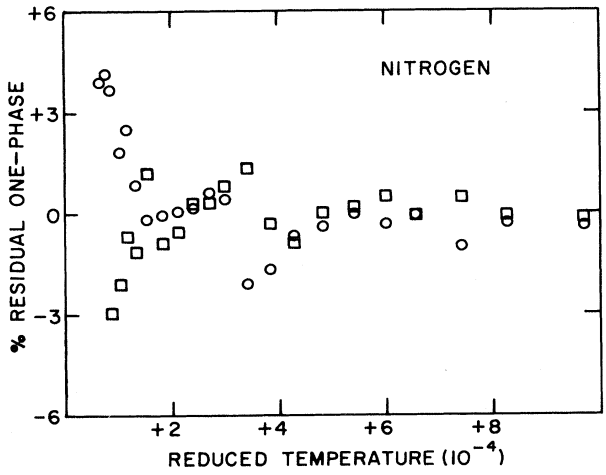


FIG. 8. Percentage residual of the power-law fit of the form $\chi_T^{\pm}=\Gamma_0^{+}t^{-\gamma}(1+\Gamma_1^{+}t^{\Delta})$, with all parameters except $\Delta$ (equal to 0.5) floating. Squares and circles represent, respectively, data from the outer and inner capacitor gaps.

### G. Cubic model analysis

Measurements which deviate significantly from their specific path due to gravity can be analyzed using a parametric model.[47–49] The restricted cubic model equation of state[35,49] transforms the temperature and density to parametric variables $r$ and $\theta$ according to the following prescription:

$$t=r(1-b^2\theta^2)\,, \tag{12}$$

$$\Delta\rho^*=r^{\beta}k\theta(1+c\theta^2)\,, \tag{13}$$

$$\Delta\mu^*=r^{\beta\delta}a\theta(1-\theta^2)\,, \tag{14}$$

where $\Delta\mu^*=(g\rho_c/P_c)(\Delta z)$ and $\Delta z=z-z_0$. Here, $z$ is the height in cm and $z_0$ is the height at which $\rho=\rho_c$ in the fluid. In the restricted cubic model, $b^2$ is assigned the value 1.2766, and $c$, 0.055. For these special values of $b^2$ and $c$ the isothermal compressibility becomes a function of $r$ only (i.e., independent of $\theta$), and the predicted amplitude ratios[26] are always maintained. This representation, which incorporates scaling, is not limited to a specific thermodynamic path. We make use of it only in a small region above the critical point, i.e, $2\times10^{-5}<t<2\times10^{-4}$, and corrections to scaling are not required. Since at each temperature our capacitance assembly gave four independent measurements of density versus chemical potential, we have, in fact, 40 data points for $N_2$ and 52 data points for Ne in this narrow temperature range. In the two-phase region are analyzed. The procedure is to solve for $r$ and $\theta$ in terms of $\Delta\rho^*$ and $t$ using Eqs. (12) and (13) for an initial set of free parameters, then fit $\Delta\mu^*$ to Eq. (14) and repeat the process. This analysis uses the same non- an initial set of free parameters, then fit $\Delta\mu^*$ to Eq. (15) and repeat the process. This analysis uses the same nonlinear least-squares-fitting routine used for the power laws. In our analysis, we make the assumption that $z_0$, the position where $\rho=\rho_c$, is at the center of the middle capacitor plate. The fact that this is not a bad assumption can be deduced from Figs. 2 and 3 for $N_2$ and their counterparts for Ne. In these figures, we see that the density as determined by the four capacitor gaps approach the average value very symmetrically as the temperature is raised from below $T_c$ to above $T_c$. Indeed, the average density of the sample is very close to $\rho_c$, within 0.15% for $N_2$ and 0.4% for Ne.

The connection between restricted cubic model parameters and the amplitudes of the power laws is $\Gamma_0^{+}=k/a$ and $B_0=k(1+c)/(b^2-1)^{\beta}$. Any temperature gradient causes its most noticeable effect near $T_c$ and should show up as a poor match between restricted cubic model parameters and power-law amplitudes. For $N_2$ we find that $a=20.4\pm0.8$ and $k=0.96\pm0.01$, which yields $B_0=1.538\pm0.016$ and $\Gamma_0^{+}=0.047\pm0.003$ (to be compared with $B_0=1.479\pm0.006$ and $\Gamma_0^{+}=0.048\pm0.001$ from power-law analysis). For Ne, $a=18.2\pm0.5$ and $k=0.945\pm0.008$, which yields $B_0=1.513\pm0.012$ and $\Gamma_0^{+}=0.052\pm0.002$ (compared to $B_0=1.425\pm0.010$ and $\Gamma_0^{+}=0.052\pm0.003$). The critical temperatures for $N_2$ and Ne are found in data analyses to be 126.2143 and 44.4789 K, in complete agreement with power-law analyses. The excellent consistency we found between the cubic model analysis and power-law analysis for $T_c$, $B_0$, and $\Gamma_0^{+}$ also indicates that there must not be any significant temperature gradient in our sample. This is the case because we do not determine $a$ directly but rather the ratio of $a$ and $g$, the gravitational constant [see Eq. (14)]. Since the values we found for $\Gamma_0^{+}$ and hence $a$ are consistent with power-law analyses, there is no significant temperature gradient to alter the "effective" gravitational constant.

### H. Compressibility in two-phase region

Our stacking capacitor assembly allows direct measurements of the compressibility of the fluid in the two-phase as well as the one-phase region. The vapor-phase compressibility can be deduced from the density difference between the top two capacitor-gap and the liquid-phase values from the lower two capacitor-gap density measurements (see Fig. 3). The vapor-phase compressibility is expected to be identical to that in the liquid phase. Since the compressibility in the two-phase region is about a factor of 5 smaller than that in the one-phase region,[26] meaningful data in the two-phase region extend over even a narrower temperature range than that in the one-phase region. Inside $|t|=1\times10^{-4}$, gravitational rounding becomes severe, at $|t|=5\times10^{-4}$, the uncertainty in the density difference between neighboring capacitor gaps due to the uncertainty in $\mathscr{C}_E$ (empty capacitance ratio) is $\sim5\%$ of the density difference. The percentage uncertainty increases rapidly as $|t|$ is increased. In Fig. 9 the $N_2$ vapor-phase compressibility in the two-phase region is plotted against the reduced temperature on a log-log scale. This figure shows that the data in the temperature range $4.5\times10^{-4}>|t|>1.5\times10^{-4}$ is consistent with a simple power law of the form

$$\chi_T^{-}=\Gamma_0^{-}t^{-\gamma^-}\,, \tag{2}$$

with $\gamma^-=\gamma^+=1.24$, and $\Gamma_0^{-}=0.010\pm0.001$. The value and uncertainty of $\Gamma_0^{-}$ is evaluated by dividing the mea-

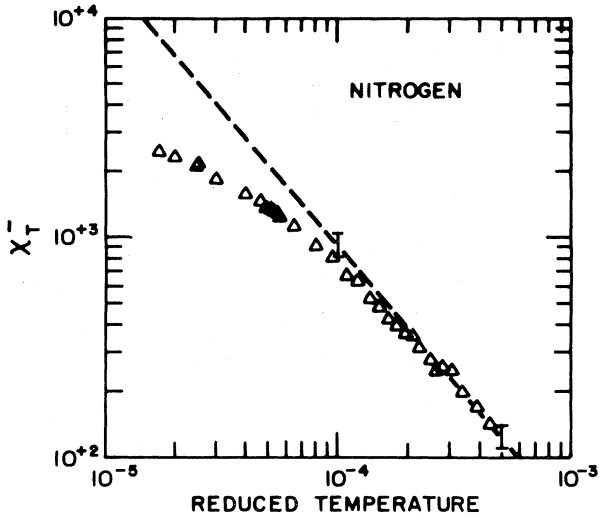


FIG. 9. Two-phase ($T<T_c$) isothermal compressibility $\chi_T^-$ as a function of reduced temperature $|t|$. The dashed line is drawn according to $\Gamma_0^-|t|^{-1.24}=0.010|t|^{-1.24}$ (with $T_c=126.2143$); the error bars shown represent an uncertainty in $\Gamma_0^-$ of $\pm 0.001$.

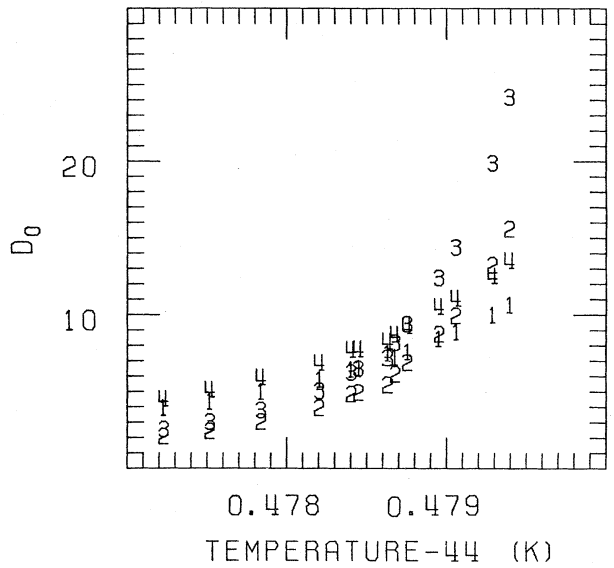


FIG. 10. Plot of $D_0=(g\rho_c/P_c)[\Delta z/|(\rho-\rho_c)/\rho_c|^{\delta}]$ for Ne with $\delta=4.82$. The symbols 1 represent the determination of $D_0$ using the density and height value of the topmost capacitor gap, and the same applies to 2, 3, and 4. At $T=T_c=44.4789$ K, we found $D_0=10\pm 3$.

sured $\chi_T^-$ value by $t^{-1.24}$ in the temperature range $4.5\times10^{-4}>|t|>1.5\times10^{-4}$. Using a similar procedure, we found $\Gamma_0^-=0.011\pm0.0015$ for Ne.

### I. Critical isotherm

On the critical isotherm our five stacked capacitor plates measure the density at four different values of chemical potential. If we write $\Delta\mu^*=g(\rho_c/P_c)\Delta z$, where $\Delta z=z-z_0$ is the height difference between a particular capacitor gap (at $z$) and the position where $\rho=\rho_c$ (at $z_0$), we can then rewrite Eqs. (3) and (4) as

$$D_0=(g\rho_c/P_c)[\Delta z/|(\rho-\rho_c)/\rho_c|^{\delta}]\ . \tag{15}$$

As in Sec. III G, we shall assume $z_0$ is at the center of the middle capacitor plate. In Fig. 10 we apply Eq. (15) to our Ne data points near $T=T_c$. The symbol "1" represents the value of $D_0$ obtained by assuming $\delta=4.82$ and using the value of density $\rho_1$ and height $z_1$ at the top gap, the symbol "2" represents the value of $D_0$ from the second gap from the top, etc. [Since Eq. (15) is expected to be valid only at $T=T_c$, in the ideal condition, we would expect the symbols 1, 2, 3, and 4 to coincide at $T=T_c$. Using the $T_c$ determined above ($T_c=44.4789$ K), we found in this procedure $D_0=10\pm3$. Following the same procedure we found $D_0=8\pm2$ for $N_2$. The uncertainty in $D_0$ is large; this is probably due to the fact that $D_0$ is extremely sensitive to any possible small error in $\rho-\rho_c$ through the large exponent $\delta$.

## IV. DISCUSSION OF RESULTS

The design of this experiment allows us to extract reliable information in the critical region. Firstly, our measurements clearly indicate over which range of temperature a power-law analysis is appropriate. Data in the gravitationally rounded region are analyzed with the restricted cubic model equation of state. Secondly, the four-capacitor setup allows for the detection of possible temperature gradient in the sample, and our special heater and heat-sinking configurations of our sample cell allow for the elimination of any significant temperature gradient.

Excellent consistency is found in the determination of $T_c$, $B_0$, and $\Gamma_0$ from the power-law analysis of order-parameter data, power-law analysis of isothermal compressibility data, and the cubic model analysis of data near $T_c$. The maximum difference in $T_c$ found for both $N_2$ and Ne in these three different analyses is 0.3 mK. The values of $B_0$ and $\Gamma_0^+$ vary less than 4% between power-law and cubic model analysis. Such consistencies lend support to the reliability of our results.

We have shown in this paper that Wegner correction-to-scaling terms of the form $B_1t^{\Delta}$ and $\Gamma_1^+t^{\Delta}$ with $\Delta\cong0.5$ are clearly needed to describe the order-parameter data in the temperature range $6\times10^{-3}>|t|>4\times10^{-4}$ and the one-phase isothermal compressibility data in the range $3\times10^{-3}>t>7\times10^{-5}$. In order to fit order-parameter data in the range $2\times10^{-2}>|t|>1.5\times10^{-3}$, the inclusion of a second correction-to-scaling term $B_2t^{2\Delta}$ is needed.

Our results are summarized in Table IV. We wish to repeat that the uncertainties quoted for the amplitudes, and hence their ratios in this table, are not the much smaller statistical uncertainties, but rather variations in their values when completely different conditions were assumed in the analysis. For both $N_2$ and Ne fluids, we found $\beta=0.327\pm0.002$; their difference from the predicted value of 0.325 is probably insignificant. It is, however, interesting to point out that we consistently found that if $\beta$ is fixed at 0.325, the fit to our data worsens. Our determination of $\gamma$ is less precise; the values we found,

TABLE IV. Summary of experimental results.

| | $N_2$ | Ne | Theory (RG) | Theory (HTS) |
|---|---|---|---|---|
| $T_0$ | 126.2143±0.0002 | 44.4789±0.0003 | | |
| $\beta$ | 0.327±0.002 | 0.327±0.002 | 0.325 | 0.325 |
| $\gamma$ | 1.233±0.01 | 1.250±0.010 | 1.240 | 1.240 |
| $\Delta$ | 0.51±0.03 | 0.49±0.05 | 0.493 | 0.49, 0.54 |
| $B_0$ | 1.479±0.006 | 1.425±0.010 | | |
| $B_1$ | 1.02±0.06 | 1.02±0.07 | | |
| $B_2$ | −2.0±0.5 | −1.6±0.6 | | |
| $\Gamma_0^+$ | 0.048±0.001 | 0.053±0.003 | | |
| $\Gamma_1^+$ | 1.07±0.06 | 1.15±0.15 | | |
| $D_0$ | 8±2 | 10±3 | | |
| $\Gamma_0^-$ | 0.010±0.001 | 0.011±0.0015 | | |
| $\Gamma_0 D_0 B_0^{\delta-1}$ | 1.71±0.5 | 2.05±0.8 | 1.75 | 1.60 |
| $\Gamma_0^+/\Gamma_0^-$ | 4.8±0.6 | 4.8±0.8 | 4.80 | 5.07 |
| $B_1/\Gamma_1^+$ | 0.95±0.13 | 0.9±0.2 | 0.85, 0.73 | |

1.233±0.01 for $N_2$ and 1.25±0.01 for Ne, are again in very good agreement with theoretical predictions. Our determinations of $\beta$ and $\gamma$ are also in very good agreement with the experiment of Hocken and Moldover[9] performed much closer to $T_c$. In their experiment the exponents were obtained by assuming a parametric equation of state in the data analysis.

For most of the data analysis we have adopted a value of 0.5 for $\Delta$, the correction exponent. We have also allowed $\Delta$ to be a free parameter in analyzing the order-parameter data, and found $\Delta=0.51\pm0.03$ for $N_2$ and 0.49±0.05 for Ne. These values are again in very good agreement with theoretical predictions.

The amplitude ratio $\Gamma_0^+/\Gamma_0^-$ in our experiment was found to be 4.8±0.6 and 4.8±0.9, respectively. These values are in excellent agreement with the theoretical values of 4.8 (RG) and 5.07 (HTS). This ratio was found by Weber[32] to be 4.8±1 and by Wallace and Meyer[33] to be 3.7 (no uncertainty was given). Our values for the ratio $\Gamma_0^+ D_0 B^{\delta-1}$ are 1.71±0.5 ($N_2$) and 2.05±0.8 (Ne), respectively; these values are again in reasonable agreement with the theoretical values of 1.75 (RG) and 1.6 (HTS). For the correction-to-scaling amplitude ratio $B_1/\Gamma_1^+$, we found 0.95±0.13 for $N_2$ and 0.9±0.2 for Ne; these values are in good agreement with the value calculated by Chang and Houghton[27] at 0.85, and that estimated by Aharony and Ahlers[28] at 0.73. If we use the $B_1$ values obtained by excluding the second correction term on the order-parameter data taken with the inner capacitor gaps, we also find very good agreement with the theoretical results. For $N_2$ we have 0.75 and for Ne, 0.78. The only other experimental determination of this ratio is the $^3$He experiment by Pittman *et al.*[17] They found values of 0.3±0.2 if two correction to scaling terms were used in the analysis, and 0.43±0.08 if one correction term was used. These ratios have also been estimated in a number of other papers by combining results from different experiments. As we have discussed in the Introduction, values obtained this way are not reliable.

The determination of the various amplitudes in this paper is independent and unbiased in the sense that no specific parametric model equation of state with either a built-in or implied connection between the amplitudes is assumed in the analysis.

To conclude, our determination of the critical exponents, correction-to-scaling exponent, and the three universal amplitude ratios are all in good agreement with current theoretical values. These agreements lend strong support to our current understanding of the behavior of fluids near the critical point both inside and outside the simple-scaling regime.

## ACKNOWLEDGMENTS

We acknowledge with thanks the help given to us by D. Furst and X. C. Mu. We acknowledge with thanks the many useful conversations throughout the course of this experiment with J. V. Sengers, H. Meyer, M. R. Moldover, S. C. Greer, and R. W. Gammon. The work reported here was done in partial fulfillment for the Ph.D. degree for one of us (M. W. P.). This work was supported in part by the Research Corporation, and the National Science Foundation—Low Temperature Physics under Grant Nos. DMR-8206109 and DMR-7927279.

*Present address: The Standard Oil Company, Research Center, 4440 Warrensville Center Road, Cleveland, Ohio 44128.

[1]L. P. Kadanoff, in *Phase Transitions and Critical Phenomena,* edited by J. C. Domb and M. S. Green (Academic, New York, 1976), Vol. 5A, Chap. 1, pp. 1—34; C. Domb, in *Phase Transitions and Critical Phenomena,* edited by J. C. Domb and M. S. Green (Academic, New York, 1974), Vol. 3, Chap. 6, pp. 357—484.

[2]K. G. Wilson and J. Kogut, Phys. Rep. 12C, 75 (1974).
[3]G. A. Baker, B. G. Nickel, and D. J. Meiron, Phys. Rev. B 17, 1365 (1978).
[4]J. C. LeGuillou and J. Zinn-Justin, Phys. Rev. Lett. 39, 95 (1977); Phys. Rev. B 21, 3976 (1976).
[5]R. Z. Roskies, Phys. Rev. B 24, 5305 (1981); B. Nickel and M. Dixon, *ibid.* 26, 3965 (1982).
[6]J. Adler, M. Moshe, and V. Privman, Phys. Rev. B 26, 3958 (1982).
[7]J. H. Chen, M. E. Fisher, and B. G. Nickel, Phys. Rev. Lett. 48, 630 (1982).
[8]B. Widom, J. Chem. Phys. 43, 3898 (1965).
[9]R. J. Hocken and M. R. Moldover, Phys. Rev. Lett. 37, 29 (1976).
[10]F. J. Wegner, Phys. Rev. B 5, 4529 (1972).
[11]M. Ley-Koo and M. S. Green, Phys. Rev. A 23, 2650 (1981).
[12]M. Ley-Koo and J. V. Sengers, in *Proceedings of the Eighth Symposium on Thermophysical Properties,* edited by J. V. Sengers (American Society of Mechanical Engineers, New York, 1982), Vol. 1, pp. 358–364.
[13]J. J. Rehr, J. Phys. A 12, L179 (1979).
[14]L. M. Stacey, B. Pass, and H. Carr, Phys. Rev. Lett. 23, 1424 (1969).
[15]D. Balzarini and K. Ohrn, Phys. Rev. Lett. 29, 840 (1972).
[16]W. T. Estler, R. Hocken, R. Charlton, and L. R. Wilcox, Phys. Rev. A 12, 2118 (1975).
[17]C. Pittman, T. Doiron, and H. Meyer, Phys. Rev. B 20, 3678 (1979).
[18]H. Guttinger and D. Cannell, Phys. Rev. A 24, 3188 (1981).
[19]D. S. Greywall and G. Ahlers, Phys. Rev. Lett. 28, 1251 (1972); Phys. Rev. A 7, 2145 (1973).
[20]This method of analysis has been used by the National Bureau of Standards (U.S.)—University of Maryland group to fit the pressure-volume-temperature data of a number of gases. See, for example, F. W. Balfour, J. V. Sengers, M. R. Moldover, and J. M. H. Sengers, Phys. Lett. 65A, 223 (1978); J. M. H. Sengers, J. S. Gallagher, F. W. Balfour, and J. V. Sengers, in *Proceedings of the Eighth Symposium in Thermophysical Properties,* edited by J. V. Sengers (American Society of Mechanical Engineers, New York, 1982), pp. 368–376.
[21]M. Ley-Koo and M. J. Green, Phys. Rev. A 16, 2483 (1977).
[22]J. Weiner, Ph.D. thesis, University of Massachusetts, 1974; J. Weiner, K. H. Langley, and N. C. Ford, Phys. Rev. Lett. 32, 879 (1974).
[23]D. Beysens and A. Bourgou, Phys. Rev. A 19, 2407 (1979); A. Bourgou and D. Beysens, Phys. Rev. Lett. 47, 257 (1981).
[24]J. V. Sengers, in *Phase Transitions: Cargese 1980,* edited by M. Levy, J. C. LeGuillou, and J. Zinn-Justin (Plenum, New York, 1982), pp. 95–135.
[25]G. P. Furrow and S. C. Greer, J. Chem. Phys. 79, 3474 (1983).
[26]A. Aharony and P. C. Hohenberg, Phys. Rev. B 13, 3081 (1976).
[27]M. C. Chang and A. Houghton, Phys. Rev. Lett. 44, 785 (1980).
[28]A. Aharony and G. Ahlers, Phys. Rev. Lett. 44, 782 (1980).
[29]M. Vicentini-Missoni, J. M. H. Levelt-Sengers, and M. S. Green, J. Res. Nat. Bur. Stand. Sec. A 73, 563 (1969).
[30]M. Barmatz, P. C. Hohenberg, and A. Kornblit, Phys. Rev. B 12, 1947 (1975).
[31]M. R. Moldover, in *Phase Transitions: Cargese 1980,* Ref. 24.
[32]L. A. Weber, Phys. Rev. A 2, 2379 (1970).
[33]B. Wallace and H. Meyer, Phys. Rev. A 2, 1563 (1970); 5, 964 (1962).
[34]P. C. Hohenberg and M. Barmatz, Phys. Rev. A 6, 289 (1972).
[35]M. R. Moldover, J. V. Sengers, R. W. Gammon, and R. J. Hocken, Rev. Mod. Phys. 51, 79 (1979).
[36]M. W. Pestak, Ph.D. thesis, Pennsylvania State University, 1983.
[37]M. H. W. Chan, Phys. Rev. B 21, 1187 (1980).
[38]M. W. Pestak and M. H. W. Chan, Phys. Rev. Lett. 46, 943 (1981).
[39]J. L. Riddle, G. T. Furukawa and H. H. Plumb, *Platinum Resistance Thermometry,* National Bureau of Standards Monograph 1260 (U.S. GPO, Washington, D.C., 1972).
[40]M. H. W. Chan, M. Ryschkewitsch, and H. Meyer, J. Low Temp. Phys. 26, 211 (1977).
[41]The absence of any anomaly near the critical point in the dielectric constant itself is required for the validity of the Calusius-Mossotti equation. This appears to be the case for nonpolar fluid (Ref. 37). A small anomaly is seen in CO, a polar fluid (Ref. 38).
[42]J. F. Ely and G. C. Straty, J. Chem. Phys. 61, 1480 (1974).
[43]O. T. Bloomer and K. N. Rao, in *Thermophysical Properties of Nitrogen Research Bulletin* (Institute for Gas Technology, Chicago, 1962), No. 18, p. 16.
[44]P. R. Bevington, *Data Reduction and Error Analysis for the Physical Sciences* (McGraw-Hill, New York, 1969).
[45]W. Rathjen and J. Straub, in *Proceedings of the Seventh Symposium of Thermophysical Properties,* edited by A. Cezairliyan (American Society of Mechanical Engineers, New York, 1977), pp. 839–850.
[46]M. R. Moldover and R. W. Gammon, J. Chem. Phys. 80, 528 (1984).
[47]P. Schofield, Phys. Rev. Lett. 22, 606 (1969).
[48]P. Schofield, J. D. Litster, and J. T. Ho, Phys. Rev. Lett. 23, 1098 (1969).
[49]J. T. Ho and J. D. Litster, Phys. Rev. B 2, 4523 (1970).